Hindawi
Scientific Programming
Volume 2021, Article ID 4034216, 7 pages
https://doi.org/10.1155/2021/4034216

Research Article

Pattern Classification-Based Analysis on Gastrointestinal Multifunctional Apparatus Guided by Ultrasound Image after Resection of Esophageal Carcinoma

Ping Chen,[1] **Wenmin Lu**,[1] **Jue Wang**,[1] **Zhanling Guo**,[1] **and Lianchang Liu**[2]

[1]*Department of Thoracic Surgery, Hengshui People's Hospital, Hengshui 053000, Hebei, China*
[2]*Operating Theatre, Hengshui Provincial People's Hospital, Hengshui 053000, Hebei, China*

Correspondence should be addressed to Ping Chen; f12041110@st.sandau.edu.cn

Received 22 June 2021; Revised 12 August 2021; Accepted 18 August 2021; Published 29 August 2021

Academic Editor: Gustavo Ramirez

To investigate the diagnostic value of ultrasound image-guided extracorporeal gastrointestinal multifunctional instrument based on pattern classification algorithm (PCA) on the physical status of patients after esophagectomy for esophageal cancer (EC), in this study, 120 esophageal cancer patients who entered our hospital for consultation and treatment from July 2019 to July 2020 were selected as the investigation subjects, and the patients were randomly divided into a control group (gastrointestinal motility drug treatment) and an observation group (gastrointestinal motility drug + extracorporeal gastrointestinal multifunctional apparatus (EGMA) therapy), with 60 cases in each group. A pattern classification method algorithm was designed for the ultrasound image characteristics of esophageal cancer tumors and applied to the clinical identification and diagnosis of postoperative status of esophageal cancer patients by the ultrasound image-guided extracorporeal gastrointestinal multifunctional instrument. The results showed that the time of exhaustion, the time of recovery of bowel sounds, and the time of the beginning of gastrointestinal peristalsis in the observation group were better than those in the control group, and the difference between the two groups was statistically significant ($P < 0.05$); the incidence of postoperative abdominal distension in the observation group was 15%, and that in the control group was 28.3%; the incidence of postoperative abdominal distension in the observation group was significantly lower than that in the control group, and the difference was statistically significant ($P < 0.05$). In conclusion, the use of EGMA guided by ultrasound image based on PCA can effectively improve the gastrointestinal function of esophageal cancer patients and significantly reduce the incidence of postoperative complications, which is worthy of clinical promotion.

1. Introduction

Esophageal cancer is one of the malignant tumors that seriously threaten human life and health. At the early stage of esophageal cancer, there are no obvious symptoms, and some patients have difficulty in swallowing and burning pain behind the sternum, so they often miss the best treatment time due to lack of attention. At the later stage of esophageal cancer, patients may have difficulty in swallowing food, and they lose weight rapidly [1, 2]. The most common clinical treatment for esophageal cancer is surgical resection, and some studies have pointed out that the 5-year survival rate of patients with esophageal cancer surgery is 40% and the 10-year survival rate is 14%–23% [3, 4]. If patients are treated and controlled in the early stage of esophageal cancer, then the 5-year survival rate after surgery will reach more than 90% [5]. Early diagnosis and treatment of patients with esophageal cancer is necessary [6, 7].

EGMA is a novel type of gastrointestinal pacing instrument to assist patients with gastrointestinal peristalsis. For patients with abdominal distension and gastrointestinal dysfunction caused by eating after surgery, gastrointestinal pacing can play a favorable therapeutic auxiliary role [8, 9]. Prior to that, the treatment of patients' gastrointestinal function was mainly based on drugs. However, drug treatment would increase the patient's gastrointestinal burden and increase the patient's psychological pressure, and the treatment effect was not very satisfactory. The emergence of EGMA solved this problem in a timely manner

[10–12]. The main working principle of EGMA is gastrointestinal pacing. It adopts advanced electronic technology to simulate the gastrointestinal biological signal of the human body. It also utilizes the electrical rhythmic activity of gastrointestinal pacing points to set appropriate pacing parameters driven by the power of radio waves of different frequencies, thus inhibiting the electrical activity of the ectopic pacing circuit or correcting the patient's abnormal gastrointestinal rhythm. Then, it can produce rhythmic contraction or progressive movement of the stomach and intestine, relieve the gastrointestinal dysfunction of the body, and promote the restoration of normal gastrointestinal function [13].

Computer technology and various medical image intelligent recognition segmentation algorithms have emerged in recent years, and automatic classification algorithms for ultrasound images can achieve automatic classification of images by extracting medical image features and training classifiers, thus improving the efficiency of ultrasound image management [14]. Image patterns are key information and a basic visual representation in images, and accurate recognition and categorization of image patterns can greatly improve the efficiency of image recognition, reduce human and material costs, and earn more time for patients to be treated. The current pattern classification algorithms for medical images have shown good image recognition effects and have good clinical research value and application prospects [15]. Therefore, in this study, we design a PCA for the ultrasound image characteristics of esophageal cancer patients and apply it to the clinical diagnosis process of ultrasound image-guided extracorporeal gastrointestinal multifunctional instrument to assess the condition of patients after esophageal cancer resection and comprehensively evaluate the clinical application value of the algorithm by observing the indexes of the two groups of patients.

2. Materials and Methods

2.1. Selection of Research Subjects. In this study, 120 patients with EC who entered our hospital for consultation and treatment from July 2019 to July 2020 were selected as the investigation subjects, among which there were 71 males and 49 females, and the average age of all patients was 41.5 ± 4.9 years. Also, all patients were randomly divided into two groups, with 60 patients in each group: the control group was treated with gastrointestinal motility drugs and the observation group was treated with EGMA on the basis of gastrointestinal motility drugs, and the efficacy of the two groups was observed, respectively.

All patients shall undergo gastrointestinal decompression without interruption after surgery. The patients in the observation group were made to lie flat on the bed and were correctly connected to the EGMA through the abdomen. Then, corresponding treatment mode was selected, the medical staff set the treatment frequency and started the treatment, 1 time/d, 10–30 min/time, and the whole course of treatment lasted 15 days.

The research had been approved by the medical ethics committee of the hospital, the patients and their families also understood the specific situation of the research, and the research had acquired the patients' consent.

Inclusion criteria were as follows: (1) patients diagnosed with EC by surgical pathology; (2) no metastasis was diagnosed by ultrasound and patients with no contraindications to surgery; (3) patients with clear consciousness who were able to cooperate with the examination; and (4) patients who did not use related gastrointestinal motility drugs before surgery.

Exclusion criteria were as follows: (1) patients with history of severe gastrointestinal diseases; (2) patients with mental illness who cannot accurately describe the condition; (3) patients with severe heart disease and patients with pacemakers; (4) patients with digestive bleeding or bleeding tendency; and (5) patients with severe liver, gallbladder, pancreas, or spleen organic diseases.

2.2. Construction of PCA. PCA is also called pattern recognition. This work is mainly based on the support vector machine under PCA, which is a new machine learning method proposed by researchers from AT&T Bell Labs led by Vapnik. When linearly separable, its hyperplane expression equation is as follows:

$$Q^i * X + a = 0, \tag{1}$$

where Q is the normalization of the hyperplane and i denotes the hyperplane number, X is the hyperplane size, and a is the hyperplane parameter. The form of the special function is as follows:

$$f(z) = Q^i * X + a. \tag{2}$$

The discriminant function is normalized, so that all samples of the two types basically satisfy $|f(z)| \geq 1$. The value $|f(z)| = 1$, which is the closest to the hyperplane. Denoting the vertical distance from the origin to the hyperplane by $\|Q\|$, then of the sample closest to the hyperplane is set to 1 such a classification interval would be $2/\|Q\|$, so the maximum classification interval is equivalent to making $\|Q\|$ (or $\|Q\|/2$) the smallest. For the expression $2/\|Q\|$ of the segmentation gap to be meaningful, all samples must satisfy the following equation.

$$X_r\left[\left(Q^i * X_r\right) + a\right] - 1 \geq 0, \quad (r = 1, 2, \ldots n). \tag{3}$$

The problem is transformed into a secondary optimization problem, which is as follows:

$$\begin{aligned} &\min \frac{1}{2}\|Q\|^2, \\ &\text{s.t. } X_r\left(Q^i ? X_r + a\right) - 1 \geq 0 \ldots \forall_r = 1 \ldots L ?. \end{aligned} \tag{4}$$

To meet the constraints in the minimization, it is necessary to introduce the Lagrangian multiplier b, $b_r \geq 0$, and the following equation is obtained:

$$\begin{aligned} M_t &= \frac{1}{2}\|Q\|^2 - b\left[y_r\left(Q^i * X_r + a\right) - 1\right] \\ &= \frac{1}{2}\|Q\|^2 - \sum_{r=1}^{L} b_r y_r\left(Q^i * X_r + a\right) + \sum_{r=1}^{L} X_r. \end{aligned} \tag{5}$$

The problem is transformed into minimizing Q and a. b is the largest, and each element of a is nonnegative. By taking

the partial derivative of Q and a on M_t and making its value equal to 0, the following equation is obtained:

$$\frac{\partial M_P}{\partial W} = 0 \Rightarrow W = \sum_{r=1}^{L} a_r X_r y_r,$$
$$\frac{\partial L_P}{\partial a} = 0 \Rightarrow \sum_{r=1}^{L} b_r y_r = 0. \tag{6}$$

The dual form dependent on b is obtained as follows:

$$M_s = \sum_{r=1}^{L} a_r - \frac{1}{2} \sum_{rh} b_r b_h y_r y_h X_r * X_h. \tag{7}$$

$T_{rh} = y_r y_h X_r * X_h$, and the equation is finally transformed into the following one:

$$\max_b \left[\sum_{r=1}^{L} b_r - \frac{1}{2} b^t T_{rh} \right]. \tag{8}$$

After W is solved again, finding b with any point can get the average solution equation of the final support vector, which is as follows:

$$b = \frac{1}{Z_S} \sum_{m \in s} b_m y_m X_s X_m. \tag{9}$$

For each newly added sample x', it can be classified through calculation of $y' = \mathrm{sgn}(W \cdot X' + b)$.

The working theory of vector linear support vector machine is introduced, which serves as the basis of ultrasound image classification. Its characteristic is that it seeks the optimal solution for a limited sample, not just the optimal solution when the sample tends to infinity. The algorithm converts the actual problem into a high-dimensional feature space through linear conversion and realizes the nonlinear discriminant function in the original space by constructing a linear discriminant function in the high-dimensional feature space. Finally, it is transformed into a quadratic optimization problem, which solves the local optimal problem in machine learning.

2.3. Observation Indicators. The indicators of exhaust time, borborygmus recovery time, and gastrointestinal peristalsis start time of the two groups of patients were followed and recorded. The two groups of patients were compared and analyzed regarding anesthesia time, free activity time, defecation, and the incidence of abdominal distension.

2.4. Statistical Methods. The research data were processed via SPSS19.0 version statistical software. Mean ± standard deviation was how measurement data were expressed, and counting data were expressed as percentage (%). One-way analysis of variance was adopted for pairwise comparison of running time. The comparisons of age, height, weight, course of disease, ratio of male to female, and diagnostic accuracy were performed by paired t-test. The difference was statistically significant at $P < 0.05$.

3. Results

3.1. Basic Information of EC Patients. Figure 1 shows the sex distribution of esophageal cancer patients, and from Figure 1, it could be concluded that among the 120 patients with esophageal cancer, there were 71 males and 49 females (Figure 1), including 33 males and 27 females in the control group and 38 males and 22 females in the experimental group. Figure 2 shows the mean age distribution of the patients in both groups. The results showed that the overall mean age of the 120 patients with esophageal cancer was 41.5 ± 4.9 years, while the mean age of the control group was 40.8 ± 5.2 years, of which the mean age of females was 44.1 ± 2.8 years and the mean age of males was 58.2 ± 3.1 years. The mean age of the experimental group was 42.1 ± 4.7 years, of which the mean age of females was 44.8 ± 4.1 years and the mean age of males was 55.7 ± 5.8 years.

The mean age and the proportion of males and females in the two groups of esophageal cancer patients were compared. It can be concluded that the mean age and male to female ratio of patients in the experimental group were not statistically significant compared with the control group ($P > 0.05$).

3.2. Preoperative Imaging Results of Some Patients. PCA was applied to screen ultrasound images of some patients, and the screening criteria were clear, very fast, and with strong adaptability. Figures 3–6 show ultrasound images of an elderly patient processed by the pattern classification algorithm. Figure 3 shows the ultrasound image of the neck longitudinal section. Figure 4 shows an ultrasound image of the cross-section of the neck, and Figure 5 shows an image of the result expression (CDFI) of blood flow detected by color Doppler ultrasound. Figure 6 shows a pulse waveform pulse Doppler (PW) image diagram.

According to the ultrasound results, the local normal wall structure of the patient's cervical esophagus disappeared, the wall was unevenly thickened, and it was hypoechoic. The distribution was not uniform. The thicker part was about 9.8 mm. The CDFI results showed that the blood flow signal was abundant, and the PW results showed that the PW probe and the low-speed high-resistance artery spectrum showed abnormalities in the patient's carotid artery spectrum. According to the above-mentioned imaging examination results, it was considered as cervical esophageal cancer, which was later confirmed by pathology.

3.3. Comparison of Borborygmus Recovery between the Two Groups. After the operation, the borborygmus recovery time of EC patients recorded by professional medical staff was compared. After surgery, the borborygmus recovery time of EC patients in the control group were (17.53 ± 4.87) hours, and that in the observation group was (7.59 ± 5.27) hours. Figure 7 shows the comparison and analysis between the two groups; the recovery time of borborygmus in the observation group was remarkably inferior to the control group, and evident differences were found ($P < 0.05$).

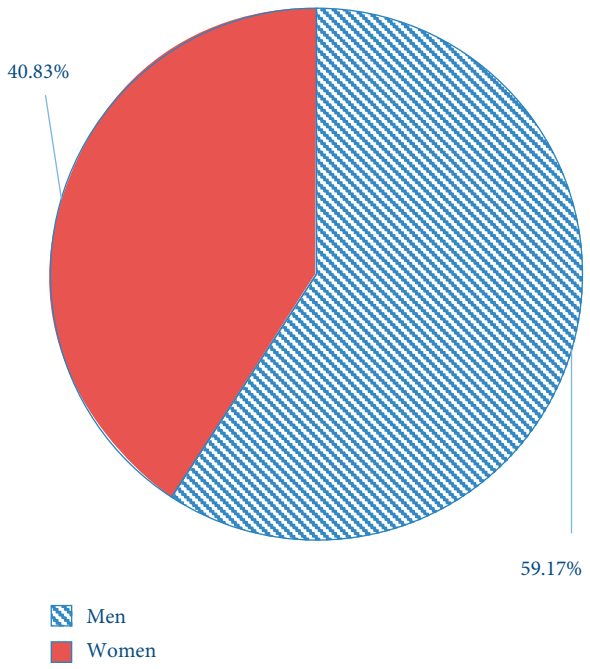

Figure 1: The gender distribution of EC patients.

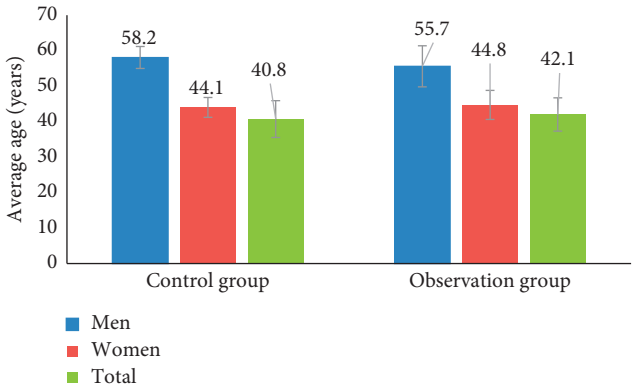

Figure 2: Comparison of the mean age of patients in the two groups.

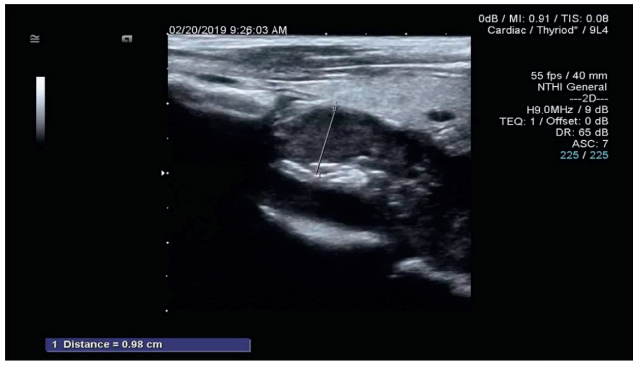

Figure 3: Longitudinal section of the neck showing obvious local thickening of the esophagus.

3.4. The Start Time of Gastrointestinal Peristalsis in the Two Groups of Patients. Figure 8 shows the start time of gastrointestinal peristalsis after the operation of the two groups

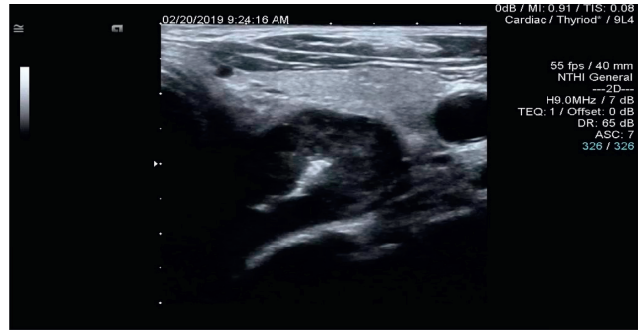

Figure 4: Cross section of neck showing thickening of esophageal wall.

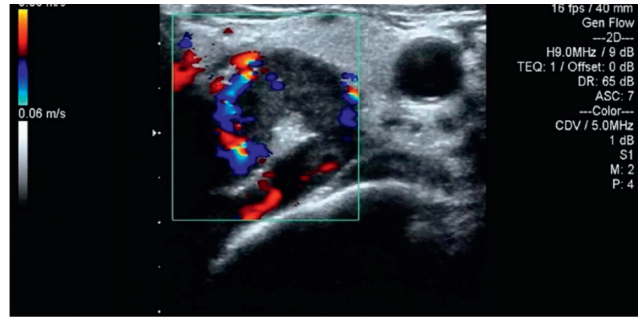

Figure 5: CDFI showing rich blood flow signals on thickened esophageal wall.

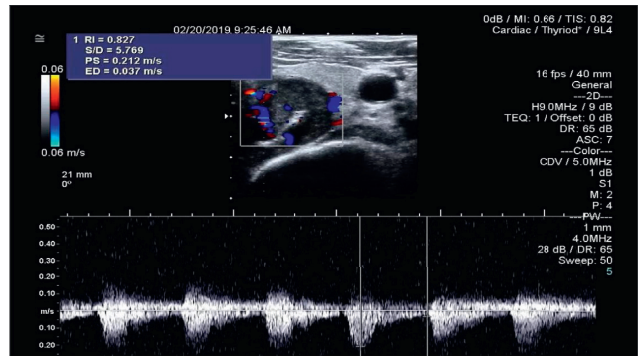

Figure 6: PW showing low-speed high-impedance spectrum.

of patients. In the control group treated with gastrointestinal drugs, the time to start gastrointestinal peristalsis after surgery was (14.8 ± 4.27) hours. The start time for gastrointestinal peristalsis after the operation in the observation group treated with EGMA was (7.1 ± 3.71) hours. For the gastrointestinal peristalsis start time, the time taken by observation group was greatly shorter in contrast to the control group ($P > 0.05$).

3.5. Comparison of the First Exhaust Time after Operation between the Two Groups. Figure 9 shows that the time for the first gastrointestinal exhaust time of the patients in the control group after the operation was (37.64 ± 5.44) hours. The first exhaust time of the observation group after

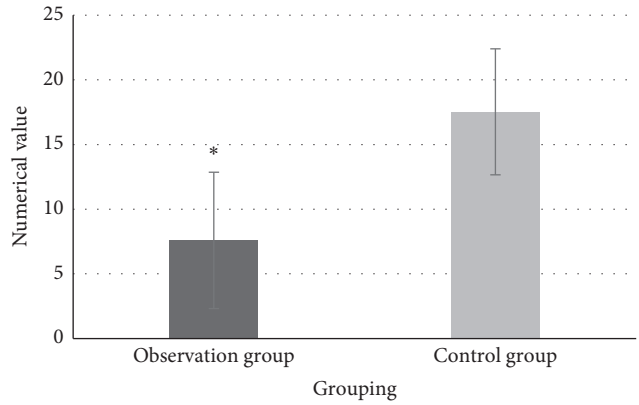

Figure 7: Comparison of borborygmus recovery time between the two groups (*indicated considerable difference relative to the control group).

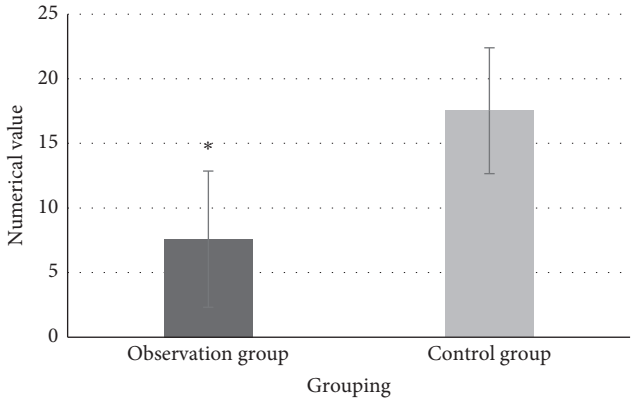

Figure 8: Start time of gastrointestinal peristalsis in the two groups (1: start time of gastrointestinal peristalsis; *meant considerable difference relative to the control group).

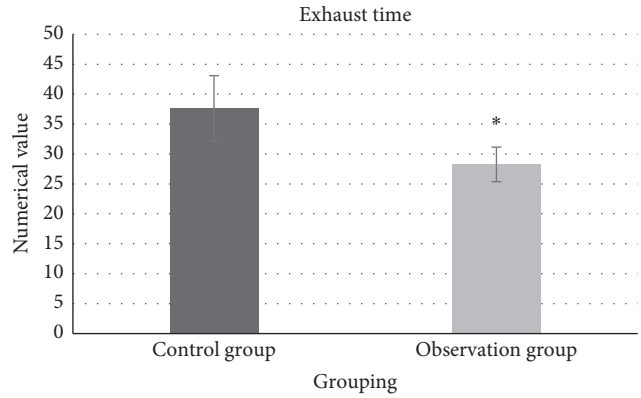

Figure 9: Comparison of the first exhaust time after operation between the two groups (*meant considerable difference relative to the control group).

operation was (28.26 ± 2.89) hours, which was evidently inferior to the control group, with very considerable difference ($P < 0.05$).

3.6. Comparison of the First Defecation Time after Operation between the Two Groups. Figure 10 shows the time for the first defecation of the two groups of patients after surgery, and the time for the first defecation in the control group treated with gastrointestinal drugs was (98.64 ± 7.65) hours. The time for the first defecation in the observation group after EGMA treatment was (72.56 ± 3.19) hours. Comparison between the two groups of patients indicated that the first defecation time of the observation group was greatly shorter versus the control group, and there was remarkable difference between them ($P < 0.05$).

3.7. Comparison of Postoperative Recovery between the Two Groups. There was no substantial difference in the anesthesia time between the two groups of patients after surgery ($P > 0.05$). After observation and recording, the time taken for the observation group to recover ambulation after the operation was (10.3 ± 1.78) days, and that for the control group was (17.1 ± 3.3) days. There were 9 cases of postoperative abdominal distension in the observation group, with a rate of 15%, and 17 cases of postoperative abdominal distension in the control group, with a rate of 28.3% (Figure 11). It can be inferred that the effect of the observation group was superior to the control group in terms of postoperative recovery and abdominal distension, and the differences were very obvious ($P < 0.05$).

4. Discussion

At present, the most common treatment for esophageal cancer is surgical resection, but the surgical resection process has a great risk, which will destroy the gastrointestinal function of the patient and then induce many complications. Therefore, the postoperative recovery process of patients is very important in the treatment of esophageal cancer, which will directly affect the prognosis of patients. It has been shown that after clinical esophagectomy, the structure of the esophagus and stomach will be temporarily altered so that the stomach is lifted into the thoracic cavity and anastomosed with the residual esophagus, and the pressure in the thoracic cavity becomes negative, which reduces the pressure gradient between the stomach and duodenum in the

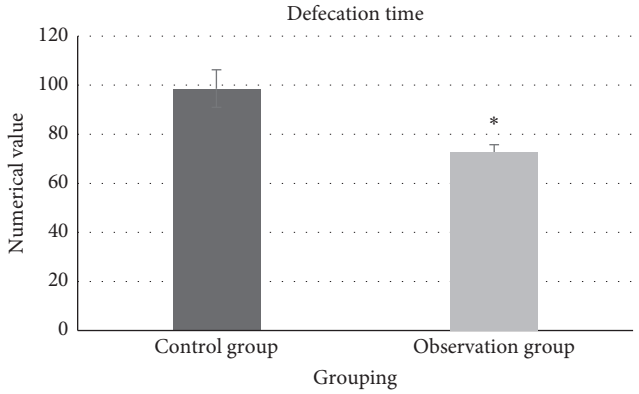

Figure 10: Comparison of first defecation time between the two groups (*meant considerable difference relative to the control group).

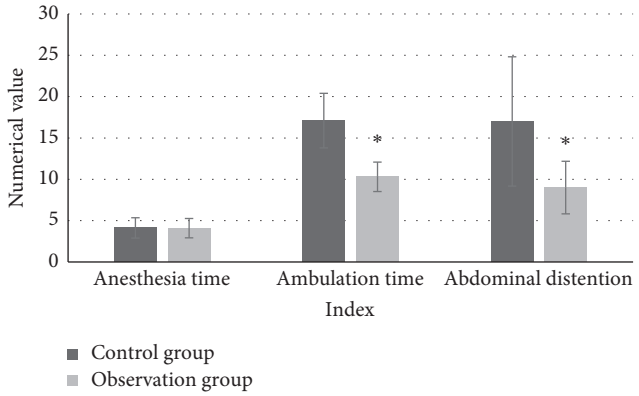

Figure 11: Comparison of postoperative recovery between the two groups (*meant considerable difference relative to the control group).

thoracic cavity and causes great pressure on the peristalsis and emptying of the gastrointestinal tract [16].

Several studies have reported on the treatment of gastrointestinal dysfunction that occurs in patients with EC after surgery. Among them, pattern classification algorithm can achieve fast screening of ultrasound images, while the hardware requirements are low and easier to achieve the effect of ultrasound images, which is the most active branch in the field of pattern recognition machine learning in recent years and one of the most mature and applied algorithms. In this research, the algorithm principle of pattern classification was applied to the screening of ultrasound images, which greatly improved the screening efficiency, was very convenient, and effectively saved the treatment time. The results showed that the recovery time of bowel sounds after surgery was 17.53 ± 4.87 hours in the control group and 7.59 ± 5.27 hours in the observation group of EC patients, the recovery time of bowel sounds in the observation group was significantly shorter than that in the control group, and there was a statistical difference between the two ($P < 0.05$). The time to start peristalsis after surgery was 14.8 ± 4.27 hours in the control group treated with gastrointestinal drugs and 7.1 ± 3.71 hours in the observation group treated with extracorporeal gastrointestinal multifunctional apparatus, and the time to start peristalsis after surgery was significantly shorter in the observation group than that in the control group ($P < 0.05$). In the control group, the time to first gastric expulsion after surgery was 37.64 ± 5.44 hours, and in the observation group, it was 28.26 ± 2.89 hours, and the time to first gastric expulsion in the control group was significantly longer than that in the observation group, with statistical differences ($P < 0.05$). In the control group, the time to first bowel movement after treatment with gastrointestinal drugs was 98.64 ± 7.65 hours, and in the observation group, the time to first bowel movement after treatment with extracorporeal gastrointestinal multifunctional instrument was 72.56 ± 3.19 hours. The first bowel movement time of the patients in the observation group was significantly shorter than that of the control group, and the two groups were statistically different ($P < 0.05$). There were 9 cases of postoperative bloating in the observation group, with an incidence of 15%, and 17 cases of postoperative bloating in the control group, with an incidence of 28.3%, so the incidence of postoperative bloating in the observation group was significantly lower than that in the control group, and there was a statistical difference between the two ($P < 0.05$), which was similar to the findings of Zhang and Zhang [17] and Kimoto et al. [18].

The results of this study confirmed that the ultrasound image-guided EGMA under pattern classification algorithm can be used for electronic pacing therapy of the gastrointestinal in patients undergoing esophageal cancer surgery, which can accelerate the recovery of the gastrointestinal function by stimulating the patient's diseased area through physiological electrical stimulation and promoting the nerve activity related to the action of the gastrointestinal tract in the patient's body. In addition, the pattern classification algorithm shows good recognition effect and speed in the process of postoperative ultrasound image recognition and classification of EC patients, which has a good application prospect in the field of ultrasound image recognition of future ultrasound image-guided EGMA.

5. Conclusion

The results show that this kind of assisted diagnosis and treatment can effectively improve the efficiency of diagnosis and treatment, and the result confirms that the EGMA can effectively promote the recovery of early gastrointestinal function of postoperative patients with EC, which has high clinical promotion value and significance. The shortcoming of this study is that the sample size of selected patients is small and there is a certain bias, and the scope of application of the study results is also small. In the subsequent study, the sample size of patients will be increased and the scope of the study will be expanded to further explore the value of EGMA in the postoperative application of esophageal cancer patients. In conclusion, the results of this paper provide some reference and significance for the clinical application of EGMA in patients with EC.

Data Availability

The data used to support the findings of this study are available from the corresponding author upon request.

Conflicts of Interest

The authors declare that they have no conflicts of interest.

References

[1] A. Dahou, M. A. Elaziz, J. Zhou, and S. Xiong, "Arabic sentiment classification using convolutional neural network and differential evolution algorithm," *Computational Intelligence and Neuroscience*, vol. 2019, Article ID 2537689, 16 pages, 2019.

[2] A. Al-Saffar, S. Awang, H. Tao, N. Omar, W. Al-Saiagh, and M. Al-Bared, "Malay sentiment analysis based on combined classification approaches and senti-lexicon algorithm," *PLoS One*, vol. 13, no. 4, Article ID e0194852, 2018.

[3] C. Guo, J. Lu, Z. Tian, W. Guo, and A. Darvishan, "Optimization of critical parameters of PEM fuel cell using TLBO-DE based on elman neural network," *Energy Conversion and Management*, vol. 183, pp. 149–158, 2019.

[4] W. Luo, Z. Zhang, T. Wen, C. Li, and Z. Luo, "Features extraction and multi-classification of sEMG using a GPU-accelerated GA/MLP hybrid algorithm," *Journal of X-Ray Science and Technology*, vol. 25, no. 2, pp. 273–286, 2017.

[5] Y. Wang, S. Sohn, S. Liu et al., "A clinical text classification paradigm using weak supervision and deep representation," *BMC Medical Informatics and Decision Making*, vol. 19, no. 1, p. 1, 2019.

[6] N. Yoshida, O. Dohi, K. Inoue et al., "Efficacy of scissor-type knives for endoscopic mucosal dissection of superficial gastrointestinal neoplasms," *Digestive Endoscopy*, vol. 32, no. 1, pp. 4–15, 2020.

[7] H.-H. Zhang, L. Yang, Y. Liu et al., "Classification of Parkinson's disease utilizing multi-edit nearest-neighbor and ensemble learning algorithms with speech samples," *BioMedical Engineering Online*, vol. 15, no. 1, p. 122, 2016.

[8] Y. Ichijo, Y. Takeda, Y. Oguma, Y. Kitagawa, H. Takeuchi, and A. Z. Doorenbos, "Physical activity among postoperative esophageal cancer patients," *Cancer Nursing*, vol. 42, no. 6, pp. 501–508, 2019.

[9] G. Okada, C. Momoki, D. Habu et al., "Effect of postoperative oral intake on prognosis for esophageal cancer," *Nutrients*, vol. 11, no. 6, p. 1338, 2019.

[10] K. Cappelli, R. Gialletti, B. Tesei et al., "Guanylin, uroguanylin and guanylate cyclase-C are expressed in the gastrointestinal tract of horses," *Frontiers in Physiology*, vol. 10, p. 1237, 2019.

[11] Z. Lv and W. Xiu, "Interaction of edge-cloud computing based on SDN and NFV for next generation IoT," *IEEE Internet of Things Journal*, vol. 7, no. 7, pp. 5706–5712, 2020.

[12] W. K. Cho, D. Oh, H. K. Kim et al., "Dosimetric predictors for postoperative pulmonary complications in esophageal cancer following neoadjuvant chemoradiotherapy and surgery," *Radiotherapy & Oncology*, vol. 133, pp. 87–92, 2019.

[13] F. Schlottmann, P. D. Strassle, A. Nayyar, F. A. M. Herbella, B. A. Cairns, and M. G. Patti, "Postoperative outcomes of esophagectomy for cancer in elderly patients," *Journal of Surgical Research*, vol. 229, pp. 9–14, 2018.

[14] T. Kawamoto, K. Nihei, K. Sasai, and K. Karasawa, "Involved-field chemoradiotherapy for postoperative solitary lymph node recurrence of esophageal cancer," *Esophagus*, vol. 15, no. 4, pp. 256–262, 2018.

[15] Y. Chen, S. Hu, H. Mao, W. Deng, and X. Gao, "Application of the best evacuation model of deep learning in the design of public structures," *Image and Vision Computing*, vol. 102, Article ID 103975, 2020.

[16] M. J. Fidler, J. A. Borgia, P. D. Bonomi, and P. Shah, "Prognostic significance of skeletal muscle loss during early postoperative period in elderly patients with esophageal cancer," *Annals of Surgical Oncology*, vol. 26, no. 12, pp. 3807-3808, 2019.

[17] Z. Zhang and H. Zhang, "Impact of neoadjuvant chemotherapy and chemoradiotherapy on postoperative cardiopulmonary complications in patients with esophageal cancer," *Diseases of the Esophagus*, vol. 30, no. 4, pp. 1–7, 2017.

[18] T. Kimoto, H. Yamazaki, G. Suzuki et al., "Local field radiotherapy without elective nodal irradiation for postoperative loco-regional recurrence of esophageal cancer," *Japanese Journal of Clinical Oncology*, vol. 47, no. 9, pp. 809–814, 2017.